ELSEVIER

Journal of Nuclear Materials 281 (2000) 15–21

journal of nuclear materials

www.elsevier.nl/locate/jnucmat

Studies on thermal expansion and XPS of urania–thoria solid solutions

S. Anthonysamy [a], G. Panneerselvam [a], Santanu Bera [b], S.V. Narasimhan [b], P.R. Vasudeva Rao [a,*]

[a] *Fuel Chemistry Division, Indira Gandhi Centre for Atomic Research, Kalpakkam 603 102, India*
[b] *Water and Steam Chemistry Laboratory, Indira Gandhi Centre for Atomic Research, Kalpakkam 603 102, India*

Received 22 February 2000; accepted 18 June 2000

Abstract

The thermal expansion characteristics of polycrystalline $(U_yTh_{1-y})O_2$ solid solutions with $y = 0.13$, 0.55 and 0.91 were determined in the temperature range from 298 to 1973 K by means of X-ray diffraction technique. For these temperatures, the average linear thermal expansion coefficients for $(U_{0.13}Th_{0.87})O_2$, $(U_{0.55}Th_{0.45})O_2$ and $(U_{0.91}Th_{0.09})O_2$ are 1.033×10^{-5}, 1.083×10^{-5} and 1.145×10^{-5} K^{-1}, respectively. The measured thermal expansion values were compared with those calculated by applying the equations for linear thermal expansion of pure urania and thoria. It was shown that the stoichiometric $(U, Th)O_2$ solid solutions are almost ideal at least up to 2000 K. The binding energies of U $4f_{7/2}$ and Th $4f_{7/2}$ electrons of $(U_{0.1}Th_{0.9})O_2$, $(U_{0.25}Th_{0.75})O_2$, $(U_{0.50}Th_{0.50})O_2$, $(U_{0.75}Th_{0.25})O_2$ and $(U_{0.90}Th_{0.10})O_2$ were experimentally determined by X-ray photoelectron spectroscopy. The result showed the presence of only U^{4+} and Th^{4+} chemical states in the stoichiometric urania–thoria solid solutions.

1. Introduction

U^{4+} and Th^{4+} have close ionic radii (0.100 and 0.105 nm, respectively) [1,2] and UO_2 and ThO_2 have the same fluorite-type structure with close lattice constants ($a = 0.54705$ and 0.55975 nm, respectively) [3]. Therefore, UO_2 and ThO_2 form a complete solid solution with cubic fluorite-type structure. The solid solutions are considered as potential fuels for advanced pressurised heavy water reactors as well as thermal breeder reactors [4]. They are stable without phase transformation up to the melting point. The lattice parameters of the solid solutions at room temperature obey the Vegard's law over the entire compositional range [3]. However, the behaviour of the solid solutions at elevated temperatures, as a function of composition, has not been clearly established. The thermal expansion of these fuel materials should be known precisely to assess the behaviour of fuel materials at high temperatures. The temperature ranges and the compositions over which the thermal expansion has been measured by various investigators [5–8] are given in Table 1. From the table it is seen that the literature data are meager on the thermal expansion of $(U, Th)O_2$ solid solutions. Hence, in the present study, the thermal expansion of $(U_{0.13}Th_{0.87})O_2$, $(U_{0.55}Th_{0.45})O_2$ and $(U_{0.91}Th_{0.09})O_2$ was measured over the temperature range from 298 to 1973 K, with a view to have more data for these solid solutions in order to elucidate their behaviour at elevated temperatures which would, in turn, contribute in complete understanding of the U–Th–O system.

Information on the binding energies of U $4f_{7/2}$ and Th $4f_{7/2}$ electrons of $(U_yTh_{1-y})O_2$ solid solutions is important to understand the chemical bonding in the solid solutions, which has a bearing on various physicochemical properties of the solid solutions. However, the data on the binding energies of cations in these solid solutions are not available in the literature. Hence, the binding energies of U $4f_{7/2}$ and Th $4f_{7/2}$ electrons of $(U_{0.1}Th_{0.9})O_2$, $(U_{0.25}Th_{0.75})O_2$, $(U_{0.50}Th_{0.50})O_2$,

* Corresponding author. Tel.: +91-4114 40 229; fax: +91-4114 40 365.
E-mail address: vasu@igcar.ernet.in (P.R. Vasudeva Rao).

0022-3115/00/$ - see front matter
PII: S0022-3115(00)00185-9

Table 1
Temperature range and the composition over which thermal expansion was measured by other investigators

References	y in $(U_yTh_{1-y})O_2$	Temperature range (K)	Technique employed
[5]	0.505	299–1273	XRD
[6]	0.1, 0.2	Room temperature to 2273	Dilatometry
[7]	0.1	Room temperature to 1273	Dilatometry
[8]	0.2	Room temperature to 1600	XRD

$(U_{0.75}Th_{0.25})O_2$ and $(U_{0.90}Th_{0.10})O_2$ were experimentally determined by X-ray photoelectron spectroscopy.

2. Experimental

2.1. Chemicals

Nuclear grade uranium dioxide (99.99%) was obtained from the Nuclear Fuel Complex, India and thorium nitrate (99.99%) was from Indian Rare Earths, India.

2.2. Sample preparation and characterization

Urania–thoria solid solutions were prepared as follows: Ammonium diuranate and thorium hydroxide were co-precipitated from a mixture of uranium and thorium nitrate solution by the addition of aqueous ammonia (uranyl nitrate was obtained by dissolving nuclear grade urania in nitric acid). The precipitate was dried and calcined at 1073 K in air for 5 h. The calcined powders were then compacted at 500 MPa into pellets of 10 mm diameter and 2–3 mm thickness by employing an electrically operated double action hydraulic press. No binder or lubricant was added for the preparation of the compacts. The compacts thus prepared were sintered at 1873 K for 6 h in a flowing argon–8 vol.% hydrogen gas mixture. The oxygen to metal ratio of the compact was fixed at 2.000 by equilibrating the compact with H_2–H_2O gas mixture having an oxygen potential of −510 kJ mol^{-1} at 1073 K till equilibrium was established between the gas phase and $(U, Th)O_2$ compact [9]. Before carrying out the thermal expansion studies, the samples were characterized for their chemical composition by elemental analyses of uranium and thorium [10,11]. About 200 mg of the oxides were dissolved in concentrated HNO_3 with a few drops of diluted HF. 1ml aliquots of this solution (pH = 2.5) were titrated against diethylenetriaminepentaacetic acid using xylenol orange as the indicator to determine the amount of thorium [10]. Then to the same aliquot acetic acid buffer was added to adjust the pH to 3.5–4. The uranium content was then determined by titrating against pyridene 2,6 dicarboxylic acid using arsenazo-1 as indicator [11]. The maximum error in the measurement of the concentration of uranium/thorium by this method is ±2%. This is equivalent to an uncertainty of ±0.01 in the mole fraction of urania/thoria in the mixed oxide, reported in this study.

2.3. Thermal expansion experiments

High temperature powder X-ray diffraction measurements were carried out using a high temperature attachment (HDK 2.4, from Johanna Otto GmbH) mounted on a wide angle goniometer of XPERT MPD system obtained from Philips, The Netherlands. The high temperature attachment consists essentially of a cylindrical vacuum tight chamber at the centre of which the sample can be mounted and heated on a tantalum strip which can be resistively heated at programmed rates. A W–3% Re/W–23% Re thermocouple, spot welded to the bottom of the strip, was used for temperature measurement. The temperature of the sample was controlled within ±1 K by using a PID controller coupled to the sensing thermocouple. The vacuum chamber was first evacuated to $\sim 10^{-3}$ Pa and then filled with high pure argon gas (containing ~ 2 ppm each of H_2O and O_2). The evacuation and filling cycle of argon was repeated for at least 4–5 times before the X-ray powder patterns could be recorded in vacuum ($\sim 10^{-5}$ Pa). Lattice parameters at different temperatures were calculated using the high angle reflections. Selected diffraction angles were determined accurately by scanning slowly across the peaks. The approximate lattice parameters calculated from the Miller indices and reflection angles were refined by the method of least-squares by using the computer programme AIDS 83 [12]. The estimated error in the lattice parameter is of the order of ±0.00005 nm.

2.4. XPS experiments

The X-ray photoelectron spectrometer used in this study is the VG ESCALAB MK200X, with 150 mm hemispherical analyzer. The analyzer chamber was evacuated by a titanium sublimation pump and an ion pump to 1.7×10^{-10} mbar during measurements. The fast entry chamber was evacuated using a turbo-molecular pump backed by rotary pump. A twin anode X-ray source is provided in the analyzer chamber for operation

with Mg Kα (1253.6 eV) or Al Kα (1486.6 eV) radiation. An ion source is also provided for sputter-etch cleaning of specimens with inert gas ions at energies up to 10 keV and beam currents of the order of 10 μA. The electron energy analyzer was operated in the constant analyzer energy (CAE) mode, where the analyzer energy is fixed during a spectrum, i.e., the analyzer allowing only electrons with a particular energy to pass through. In this study, the spectra were collected using Al Kα X-ray source and with 20 eV pass energy of the analyzer. The data acquisition and processing were carried out using the Eclipse software. The instrument was calibrated with Au $4f_{7/2}$ line at 84.0 eV with 1.6 eV FWHM [13] for the specimen of Au film on Si substrate [14].

3. Results and discussion

3.1. Thermal expansion of urania–thoria solid solutions

The room temperature lattice parameters observed for the solid solutions, viz., 0.5581 for $(U_{0.13}Th_{0.87})O_2$, 0.5530 for $(U_{0.55}Th_{0.45})O_2$, and 0.5482 nm for $(U_{0.91}Th_{0.09})O_2$, are in good agreement with the literature values [3]. The variation of lattice parameter, a, with temperature measured in this study is given by the following equations:

For $(U_{0.13}Th_{0.87})O_2$,

$$a_T = 0.55690 + 3.93301 \times 10^{-6} \times T + 8.0665 \times 10^{-10} \times T^2 \pm 8.4519 \times 10^{-5}. \quad (1)$$

For $(U_{0.55}Th_{0.45})O_2$,

$$a_T = 0.55201 + 3.36692 \times 10^{-6} \times T + 1.15537 \times 10^{-9} \times T^2 \pm 1.31748 \times 10^{-4}. \quad (2)$$

For $(U_{0.91}Th_{0.09})O_2$,

$$a_T = 0.54727 + 3.00954 \times 10^{-6} \times T + 1.4387 \times 10^{-9} \times T^2 \pm 2.76039 \times 10^{-4}. \quad (3)$$

The above equations were obtained by the least-squares method and the equations are valid in the temperature range from 298 to 1973 K. A generalized equation for the lattice parameter of $(U_yTh_{1-y})O_2$ solid solutions as a function of both temperature and composition of the solid solutions is given below:

$$a_{T,y} = [0.0455 \times 10^{-5} \times y^2 - 0.1657 \times 10^{-5} \times y + 0.4141 \times 10^{-5}] \times T + [-0.0555 \times 10^{-9} \times y^2 - 0.8680 \times 10^{-9} \times y + 0.6947 \times 10^{-9}] \times T^2 + [-0.002 \times y^2 - 0.0103 \times y + 0.5583]. \quad (4)$$

Fig. 1 shows the measured lattice parameters of $(U_{0.13}Th_{0.87})O_2$, $(U_{0.55}Th_{0.45})O_2$ and $(U_{0.91}Th_{0.09})O_2$ solid solutions at various temperatures. From the figure it is observed that the lattice parameter of all the solid solutions increases progressively with increasing temperature as expected. Kempter and Elliott [5] have measured the thermal expansion of urania–thoria solid solutions containing 50.5 mol% urania over the temperature range from 299 to 1273 K by XRD technique and reported an expression for the variation of lattice parameter as a function of temperature. The fitted line of lattice parameter values computed from this expression is also shown in Fig. 1 for the purpose of comparison. Momin et al. [8] have measured the linear thermal expansion of $(U_{0.2}Th_{0.8})O_2$ over the temperature range from room temperature to 1600 K by XRD technique. Their results are also shown in Fig. 1 for comparison. The values of lattice parameters for $(U_{0.5}Th_{0.5})O_2$, measured at various temperatures by Kempter and Elliott [5] as well as those for $(U_{0.2}Th_{0.8})O_2$ measured by Momin et al. [8] lie between the values for $(U_{0.13}Th_{0.87})O_2$ and $(U_{0.55}Th_{0.45})O_2$ measured in this study. In addition, the trend in the variation of lattice parameters of $(U, Th)O_2$ solid solutions with respect to composition measured by Kempter and Elliott [5], Momin et al. [8] as well as by the present study is as expected, even though the rate of change of lattice parameter with temperature is different in the case of results reported by Momin et al. [8].

The percentage linear thermal expansion was computed using the following expression:

$$\text{Expansion } \% = \{(a_T - a_{298})/a_{298}\} \times 100, \quad (5)$$

from the temperature variation of lattice parameter in the range from 298 to 1973 K. In the above expression, a_T represents the lattice parameter at temperature T and a_{298} the value at room temperature. These values were fitted in to second order polynomials and the expressions are given below:

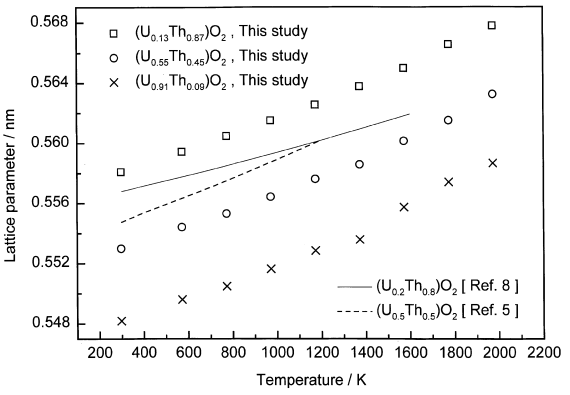

Fig. 1. Lattice parameters of urania–thoria solid solutions as a function of temperature.

For $(U_{0.13}Th_{0.87})O_2$,

$$\text{Expansion }\% = -0.17468 + 6.40888 \times 10^{-4} \times T + 1.67932 \times 10^{-7} \times T^2 \pm 0.01487. \quad (6)$$

For $(U_{0.55}Th_{0.45})O_2$,

$$\text{Expansion }\% = -0.08337 + 4.53933 \times 10^{-4} \times T + 2.65283 \times 10^{-7} \times T^2 \pm 0.01981. \quad (7)$$

For $(U_{0.91}Th_{0.09})O_2$,

$$\text{Expansion }\% = -0.07368 + 3.96778 \times 10^{-4} \times T + 3.17679 \times 10^{-7} \times T^2 \pm 0.05176. \quad (8)$$

A generalized equation for the percentage linear thermal expansions of $(U_yTh_{1-y})O_2$ solid solutions as a function of both temperature and composition of the solid solutions is given below:

$$\alpha = [0.3671 \times 10^{-3} \times y^2 - 0.6948 \times 10^{-3} \times y + 0.7250 \times 10^{-3}] \times T + [-0.1106 \times 10^{-6} \times y^2 + 0.3070 \times 10^{-6} \times y + 0.1299 \times 10^{-6}] \times T^2 + [-0.2442 \times y^2 + 0.3835 \times y - 0.2204]. \quad (9)$$

The percentage linear thermal expansions computed from the above fit equations are shown in Fig. 2 along with the values measured in this study. The percentage thermal expansion of all the solid solutions increases progressively with increasing temperature nearly independent of composition up to 1200 K. Fig. 3 compares the linear thermal expansion data obtained in this study with the data available in the literature. The linear thermal expansion of urania and thoria are also shown in the figure for the purpose of comparison. From the figure it is seen that the agreement between our results and the results reported by both Springer et al. [6] as well as Turner and Smith [7] is excellent. It is also observed that the linear thermal expansion of urania, thoria and urania–thoria solid solutions are almost identical up to 1200 K. Above 1200 K, the values of linear thermal expansion of urania–thoria solid solutions lie between those for pure urania and thoria.

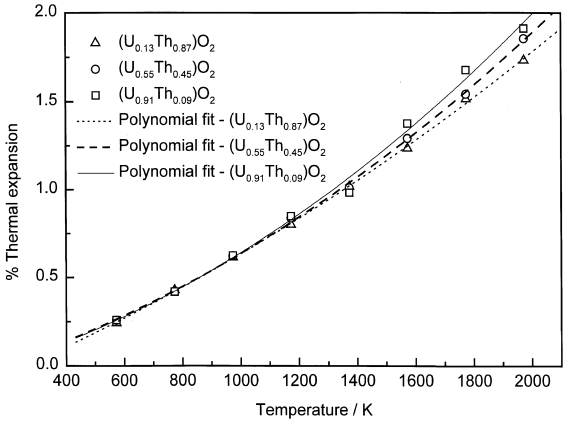

Fig. 2. Percentage linear thermal expansion of urania–thoria solid solutions.

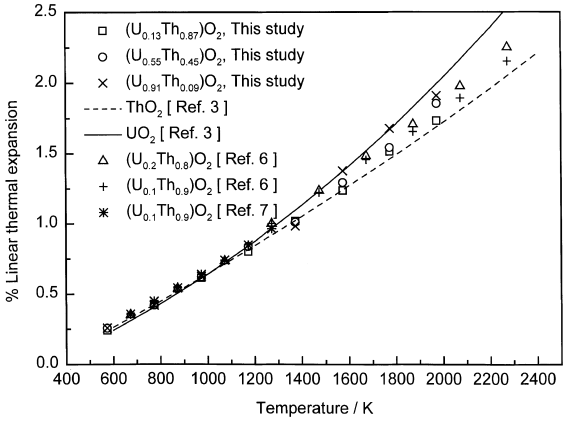

Fig. 3. Percentage linear thermal expansion of urania–thoria solid solutions measured in this study along with other data available in the literature.

The instantaneous linear thermal expansion coefficients $[\alpha = (1/a_0)(\partial a/\partial T)]$ were obtained by taking the first derivative of Eqs. (1)–(3). The following equations for α were obtained for $(U, Th)O_2$ solid solutions.

For $(U_{0.13}Th_{0.87})O_2$,

$$\alpha = 7.0471 \times 10^{-6} + 2.8907 \times 10^{-9} \times T. \quad (10)$$

For $(U_{0.55}Th_{0.45})O_2$,

$$\alpha = 6.0885 \times 10^{-6} + 4.1786 \times 10^{-9} \times T. \quad (11)$$

For $(U_{0.91}Th_{0.09})O_2$,

$$\alpha = 5.4900 \times 10^{-6} + 5.2489 \times 10^{-9} \times T. \quad (12)$$

The coefficients of average linear thermal expansion, $\bar{\alpha}, (\bar{\alpha} = (1/a_0) \times (a_T - a_{298})/(T - 298))$ derived from Eqs. (1)–(3) are given by the following expressions:

For $(U_{0.13}Th_{0.87})O_2$,

$$\bar{\alpha} = 7.4779 \times 10^{-6} + 1.4454 \times 10^{-9} \times T. \quad (13)$$

For $(U_{0.55}Th_{0.45})O_2$,

$$\bar{\alpha} = 6.7111 \times 10^{-6} + 2.0893 \times 10^{-9} \times T. \quad (14)$$

For $(U_{0.91}Th_{0.09})O_2$,

$$\bar{\alpha} = 6.2721 \times 10^{-6} + 2.6245 \times 10^{-9} \times T. \quad (15)$$

For the temperature range from 298 to 1973 K, the values of the average linear thermal expansion coefficients for $(U_{0.13}Th_{0.87})O_2$, $(U_{0.55}Th_{0.45})O_2$ and

$(U_{0.91}Th_{0.09})O_2$ are 1.033×10^{-5}, 1.083×10^{-5} and 1.145×10^{-5} K^{-1}, respectively.

Based on their thermal expansion measurements, Kempter and Elliott [5] suggested that urania–thoria solid solutions become less ideal as the temperature increases. However, Aitken et al. [15] measured the activity of UO_2 in solid solutions of $(U_yTh_{1-y})O_2$ by the transpiration method and suggested that the stoichiometric urania–thoria solid solutions are ideal at temperatures around 1573 K. A comparison of the percentage linear thermal expansion measured in this study with those calculated by applying the equations for linear thermal expansion of pure urania and thoria (Figs. 4–6) indicates that stoichiometric $(U, Th)O_2$ solid solutions are almost ideal at least up to 2000 K. In addition, the room temperature lattice parameter of the solid solutions obeys the Vegard's law. This conclusion is further supported by the fact that the enthalpy increments of $(U_{0.1}Th_{0.9})O_2$, $(U_{0.5}Th_{0.5})O_2$ and $(U_{0.9}Th_{0.1})O_2$ measured in our laboratory [16] over the temperature range from 473 to 973 K were found to obey the Neumann–Kopp's molar additivity rule.

3.2. Binding energies

U $4f_{7/2}$ and Th $4f_{7/2}$ photoelectron spectra for $(U_{0.1}Th_{0.9})O_2$, $(U_{0.25}Th_{0.75})O_2$, $(U_{0.5}Th_{0.5})O_2$, $(U_{0.75}Th_{0.25})O_2$, and $(U_{0.9}Th_{0.1})O_2$ were recorded to understand the chemical state of uranium and thorium in the mixed oxides and the change in its electronic structure due to formation of the solid solution. Figs. 7 and 8 show the photoelectron spectra of the mixed oxides. The peak positions, peak widths and the satellite positions in the photoelectron spectra are shown in Table 2. From this table it is clear that these parameters are not changed significantly from the values for pure urania and thoria. The peak positions indicate that both uranium and thorium are in +4 state. The increase in peak width

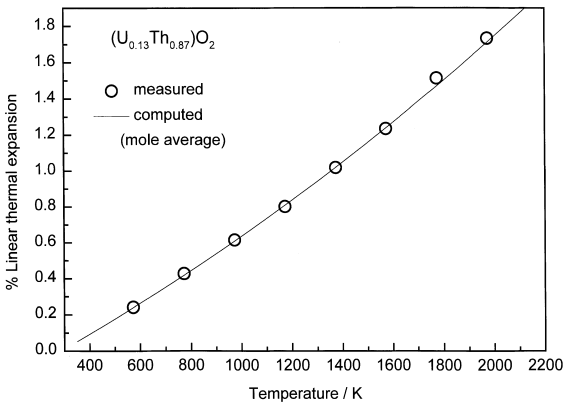

Fig. 4. Measured and computed thermal expansion of $(U_{0.13}Th_{0.87})O_2$.

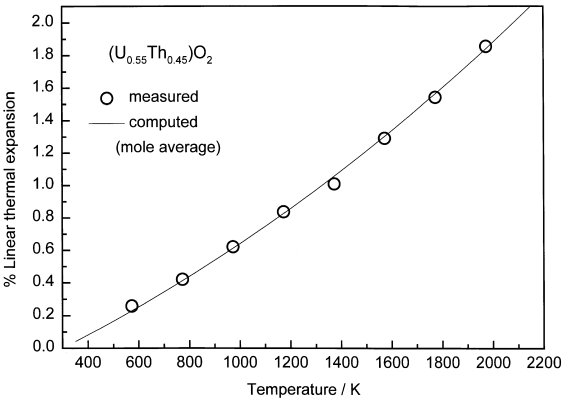

Fig. 5. Measured and computed thermal expansion of $(U_{0.55}Th_{0.45})O_2$.

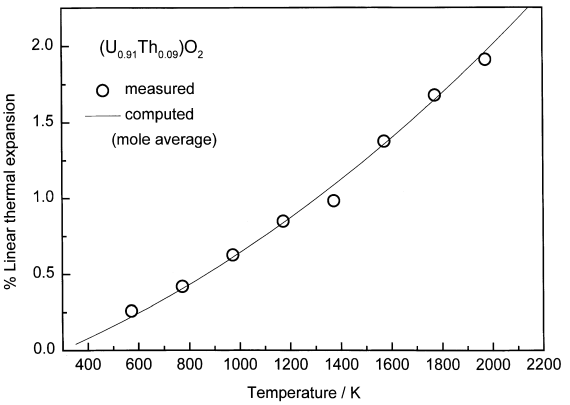

Fig. 6. Measured and computed thermal expansion of $(U_{0.91}Th_{0.09})O_2$.

is usually associated with the multiple oxidation states of the element. However, in the present study, the peak is not so wide to predict the presence of any multiple oxidation states of uranium or thorium in the solid solutions. The small change in the peak width observed in the present study for the solid solutions may be due to change in the chemical environment of the emitting atoms. Urania and thoria have the fluorite crystal structure and the mixed oxides also have the same crystal structure with uranium and thorium distributed randomly in the metal sites. In the forbidden gap of the band structure of thoria, U-bands are introduced during the formation of solid solutions. Hence, in the mixed oxide, a mixed band of uranium and thorium is developed and this influences each other to broaden the band. The binding energies of U $4f_{7/2}$ and Th $4f_{7/2}$ electrons in $(U_{0.1}Th_{0.9})O_2$, $(U_{0.25}Th_{0.75})O_2$, $(U_{0.5}Th_{0.5})O_2$, $(U_{0.75}Th_{0.25})O_2$, and $(U_{0.9}Th_{0.1})O_2$ solid solutions experimentally determined in this study are given in Table 2. The results indicate that uranium is in +4 oxidation state and thorium in +4 state in all the solid solutions as

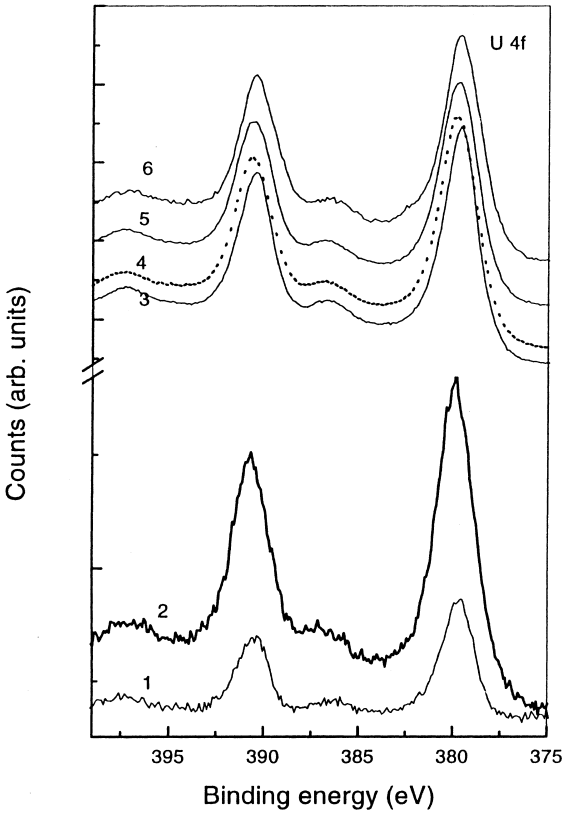

Fig. 7. U 4f photoelectron spectra for $(U_yTh_{1-y})O_2$ solid solutions: (1) $y = 0.1$, (2) $y = 0.25$, (3) $y = 1$, (4) $y = 0.9$, (5) $y = 0.75$, and (6) $y = 0.5$.

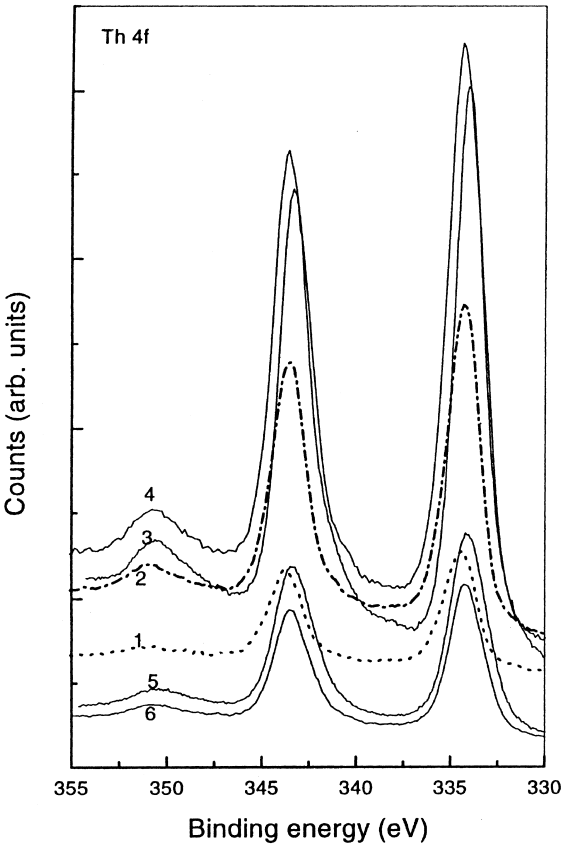

Fig. 8. Th 4f photoelectron spectra for $(U_yTh_{1-y})O_2$ solid solutions: (1) $y = 0.9$, (2) $y = 0.75$, (3) $y = 0$, (4) $y = 0.5$, (5) $y = 0.1$, and (6) $y = 0.25$.

identified from binding energy (379.9 eV for U $4f_{7/2}$ and 334.0 eV for Th $4f_{7/2}$) and satellite peak positions [17–19]. The 4f photoelectron peaks of uranium or thorium oxides are associated with satellite peaks due to the transition involving U–O or Th–O bonding bound to the empty states above the Fermi level during photoemission. The energy involved for such transitions is different for different oxidation states of uranium or thorium. In the case of U^{+4}, the satellite peak appears at 6.8 eV (Table 2), whereas for U^{+6} state, the satellite peak appears at 4.4 eV [17–19]. For Th^{+4} state, the satellite peak is seen at 7.3 eV (Table 2). Hence, not only the binding energy, but also the satellite peak positions are found to be characteristic of the oxidation state of the elements. In the present study, the presence of a satellite at 7.0–7.4 eV for (U, Th) mixed oxide of each composition, indicates that thorium is +4 oxidation state in

Table 2
Binding energy of specified atomic levels for $(U_yTh_{1-y})O_2$ solid solutions

y in $(U_yTh_{1-y})O_2$	BE[a] of U $4f_{7/2}$ (eV)	FWHM of U $4f_{7/2}$ (eV)	U$4f_{7/2}$ satellite (eV)	BE of Th $4f_{7/2}$ (eV)	FWHM of Th $4f_{7/2}$ (eV)	Th $4f_{7/2}$ satellite (eV)	References
1.00	379.9	2.2	6.8				[17–19]
0.90	379.9	2.4	6.5	334.2	2.1	7.4	This study
0.75	379.9	2.4	6.7	334.0	2.1	7.1	This study
0.50	379.9	2.4	6.8	334.1	2.2	7.0	This study
0.25	379.9	2.4	6.4	334.1	2.2	7.3	This study
0.10	379.8	2.3	6.5	334.2	2.3	7.1	This study
0.00				333.8	1.8	7.3	[18,19]

[a] Binding energy.

them. Similarly, the absence of a satellite at 4.4 eV and the presence of a satellite at 6.4–6.8 eV for (U, Th) mixed oxides indicate that the oxidation state of uranium in them is +4.

4. Conclusion

The average linear thermal expansion coefficients for $(U_{0.13}Th_{0.87})O_2$, $(U_{0.55}Th_{0.45})O_2$ and $(U_{0.91}Th_{0.09})O_2$ were measured to be 1.033×10^{-5}, 1.083×10^{-5} and 1.145×10^{-5} K^{-1}, respectively, in the temperature range between 298 and 1973 K. Based on the results of calorimetric studies [16], thermal expansion studies and other thermodynamic measurements on urania–thoria solid solutions [15], it is suggested that stoichiometric urania–thoria solid solutions are nearly ideal at least up to 2000 K. XPS study indicates that uranium and thorium are in +4 oxidation state in all the solid solutions as identified from binding energy (379.9 eV for U $4f_{7/2}$ and 334.0 eV for Th $4f_{7/2}$) and satellite peak positions.

References

[1] R.D. Shannon, C.T. Prewitt, Acta Crystallogr. B 25 (1969) 925.
[2] R.D. Shannon, Acta Crystllogr. A 32 (1976) 751.
[3] J. Belle, R.M. Berman, Thorium Dioxide: Properties and Nuclear Applications, DOE/NE-0060, 1984, p. 74.
[4] C. Ganguly, in: P. Vincenzini (Ed.), High Tech Ceramics, Elsevier, Amsterdam, 1987, p. 2887.
[5] C.P. Kempter, R.O. Elliott, J. Chem. Phys. 30 (6) (1959) 1524.
[6] J.R. Springer, E.A. Eldridge, M.V. Goodyear, T.R. Wright, J.F. Lagedrost, BMI-X-10210, 1967.
[7] D.N. Turner, P.D. Smith, Australian Atomic Energy Commission Report AAEC/E183, 1967.
[8] A.C. Momin, E.B. Mirza, M.D. Mathews, J. Nucl. Mater. 185 (1991) 308.
[9] S. Anthonysamy, K. Nagarajan, P.R. Vasudeva Rao, J. Nucl. Mater. 247 (1997) 273.
[10] E. Celon, S. Degetto, G. Marangoni, L. Baracco, Talanta 26 (1979) 160.
[11] R. Pribil, V. Vaseley, Talanta 10 (1963) 899.
[12] D.E. Appleman, H.T. Evans, Indexing and least-squares refinement of powder diffraction data, NIST Document No. PB-216188, 1973.
[13] D.K. Sarkar, Santanu Bera, S. Dhara, K.G.M. Nair, S.V. Narasimhan, S. Chowdhury, Appl. Surf. Sci. 120 (1997) 159.
[14] C.J. Powell, Surf. Interface Anal. 23 (1995) 121.
[15] E.A. Aitken, J.A. Edwards, R.A. Joseph, J. Phys. Chem. 70 (4) (1966) 1084.
[16] S. Anthonysamy, Jose Joseph, P.R. Vasudeva Rao, J. Alloys Compounds 299 (2000) 112.
[17] S. Bera, S.K. Sali, S. Sampath, S.V. Narasimhan, V. Venugopal, J. Nucl. Mater. 255 (1998) 26.
[18] B.W. Veal, D.J. Lam, H. Diamond, H.R. Hoekstra, Phys. Rev. B 15 (6) (1977) 2929.
[19] B.W. Veal, D.J. Lam, Phys. Rev. B 10 (12) (1974) 4902.